

# On the finite size mass shift formula for stable particles

Yoshiaki Koma and Miho Koma <sup>1</sup>

*Max-Planck-Institut für Physik, Föhringer Ring 6, D-80805, München, Germany*

---

## Abstract

Lüscher's finite size mass shift formula in a periodic finite volume, involving forward scattering amplitudes in the infinite volume, is revisited for the two stable distinguishable particle system. The generalized mass shift formulae for the boson and fermion are derived in the boson-boson and fermion-boson systems, respectively. The nucleon mass shift formula is given in the nucleon-pion system and the relation to the computation within chiral perturbation theory is discussed.

---

## 1 Introduction

Nowadays the control of finite volume effects in lattice QCD simulations with dynamical fermions becomes a more important issue in order to determine the hadron spectrum precisely. Applications of chiral perturbation theory (ChPT) [1] to the measured spectrum on the lattice have been done not only to achieve the chiral extrapolation [2,3], but also to find its finite volume dependence towards the thermodynamic limit [4,5,6,7,8].

In this context, Lüscher's formula, relating the mass shift in finite volume with periodic boundary conditions to forward elastic scattering amplitudes in infinite volume, provides us with an elegant tool for such a purpose [9]. In the latter reference Lüscher presented a rigorous proof of his formula for the case of a self-interacting boson to all orders in perturbation theory [10]. By writing the difference of the masses between in finite and infinite volumes as  $\Delta m(L) = M(L) - m$  with the spatial box of the size  $L^3$ , the formula is given by

---

<sup>1</sup> present address: DESY, Theory Group, Notkestrasse 85, D-22603 Hamburg, Germany

$$\Delta m(L) = -\frac{3}{8\pi mL} \left[ \frac{\lambda^2}{4\nu_B} e^{-\frac{\sqrt{3}}{2}Lm} + \int_{-\infty}^{\infty} \frac{dq_0}{2\pi} e^{-L\sqrt{q_0^2+m^2}} F(iq_0) \right] + O(e^{-\sqrt{3/2}Lm}), \quad (1)$$

where  $F(\nu)$  is the forward scattering amplitude ( $\nu = iq_0$  denotes the crossing variable), which has poles at  $\nu = \pm\nu_B$  with  $\nu_B = m/2$ . The coupling  $\lambda$  is then defined by the relation

$$\lim_{\nu \rightarrow \pm\nu_B} (\nu^2 - \nu_B^2) F(\nu) = \frac{\lambda^2}{2}. \quad (2)$$

One may ask if one can immediately generalize this formula to a theory describing the interaction of two stable particles  $A$  and  $B$  (or multiplets thereof) of different masses,  $m_A$  and  $m_B$ , respectively. One may find that the r.h.s. of Eq. (1) can be expressed by using only the second term if the integral path is extended to the complex  $q_0$  plane such as  $-\infty + i\zeta \rightarrow +\infty + i\zeta$  with  $m/2 < \zeta < m$ . In fact, the shift of the integral path back to the real  $q_0$  axis ( $-\infty \rightarrow +\infty$ ) picks up a residue associated with  $F(\nu)$  at the pole  $\nu = +\nu_B$ , which leads to the first term of Eq. (1). In this sense, we may call the first term in Eq. (1) *the pole term*. Then, we may speculate that the asymptotic formula for the  $A$ -particle mass shift for the case  $m_A \gg m_B$  is written as

$$\begin{aligned} \Delta m_A &\stackrel{?}{\approx} -\frac{3}{8\pi m_A L} \int_{-\infty+i\zeta}^{\infty+i\zeta} \frac{dq_0}{2\pi} e^{-L\sqrt{q_0^2+m_B^2}} F_{AB}(iq_0) \\ &= -\frac{3}{8\pi m_A L} \left[ \frac{\lambda^2}{4\nu_B} e^{-L\sqrt{m_B^2-\nu_B^2}} + \int_{-\infty}^{\infty} \frac{dq_0}{2\pi} e^{-L\sqrt{q_0^2+m_B^2}} F_{AB}(iq_0) \right], \quad (3) \end{aligned}$$

with  $F_{AB}(\nu)$ , the forward scattering amplitude for the  $A+B \rightarrow A+B$  process, and in this case  $\nu_B = m_B^2/2m_A$ . For instance, by identifying  $A$  with the nucleon and  $B$  with the pion, and exploiting the residue of  $F_{N\pi}(\nu)$  at  $\nu = +\nu_B$ , one would then reproduce the nucleon mass shift formula presented by Lüscher in his Cargese lectures [9].

Among the applications of ChPT, the QCDSF-UKQCD collaboration estimated the finite volume effect on the nucleon mass from data in  $N_f = 2$  lattice QCD [6], applying the mass shift formula derived within ChPT. Along the way, they found however, when expressing their formula in terms of  $F_{N\pi}(\nu)$  in the same order of ChPT, that the factor of the pole term is twice larger than that of Lüscher's in Ref. [9], although the rest is the same. There seems to be no mistake in the formula in Ref. [6], at least within the infrared regularization scheme [1]. On the other hand, Lüscher's formula being considered as general such that it can also be applicable to ChPT at any orders, this discrepancy poses a structural question.

In this paper, we thus investigate the mass shift formula for the interacting two stable particle system along the lines of Lüscher's proof for a self-interacting bosonic theory. We will not assume  $m_A \gg m_B$  (as in the physical case above) because this would obscure the general structure of the formula, so that we will keep terms which would be relevant if the masses were close. In Sect. 2, we first describe the result on the generalized mass shift formulae for the boson and fermion in the boson-boson and fermion-boson systems, respectively. In Sect. 3, we then provide a part of the derivation by selecting a typical diagram for the self energy in the two particle system. We discuss the nucleon mass shift formula in the  $N$ - $\pi$  system in Sect. 4. A summary is given in Sect. 5. Notations used in this paper are summarized in Appendix A.

## 2 Asymptotic formulae for finite size mass shift

In this section, we describe the result on the generalized mass shift formulae for the boson and fermion in the boson-boson and fermion-boson systems, respectively.

The physical mass of a stable particle is given by the position of the pole of the propagator of an asymptotic field. In the framework of perturbation theory the pole is shifted from the bare one due to the self energy arising from polarization effects from the virtual particles. In finite volume, the expressions for the self energy involve sums over discrete spatial loop momenta,  $\vec{q}(L) = 2\pi\vec{n}/L$  ( $\vec{n} \in \mathbb{Z}^3$ ), instead of integrals. By using the Poisson summation formula, such a summation can be rewritten again as an integral with another summation over integer vectors  $\vec{m} \in \mathbb{Z}^3$  and an exponential factor depending on  $L$ :

$$\frac{1}{L^3} \sum_{\vec{n} \in \mathbb{Z}^3} \int \frac{dq_0}{2\pi} f(q_0, \vec{q}(L)) = \sum_{\vec{m} \in \mathbb{Z}^3} \int \frac{d^4q}{(2\pi)^4} e^{-iL\vec{m}\cdot\vec{q}} f(q_0, \vec{q}), \quad (4)$$

where  $f(q)$  is a function composed of propagators and vertex functions. Then, the difference of the self energies between the finite and infinite volumes, appearing in the definition of the mass shift as described below, can be defined by the sum over  $|\vec{m}| \neq 0$ , since  $|\vec{m}| = 0$  corresponds to the integral in infinite volume [11]. The asymptotic formula at large  $L$ , which is of our interest, is given by the contribution of  $|\vec{m}| = 1$ . (next leading contribution is  $|\vec{m}| = \sqrt{2}$ .) In this case, the exponential factor in Eq. (4) is reduced to  $2 \sum_{i=1}^3 \cos(Lq_i)$ .

$$\Sigma_L(p) - \Sigma(p) = \frac{1}{2} \left( \begin{array}{c} \text{Diagram (a1)} \\ \text{Diagram (a2)} \end{array} \right) \quad (\text{a1, a2})$$

$$+ \begin{array}{c} \text{Diagram (b1)} \end{array} \quad (\text{b1})$$

$$+ \frac{1}{2} \left( \begin{array}{c} \text{Diagram (c1)} \\ \text{Diagram (c2)} \end{array} \right) \quad (\text{c1, c2})$$

Fig. 1. Self-energy diagrams which contribute to the mass shift formula in the  $\phi_A$ - $\phi_B$  system. A solid line with an empty circle corresponds to the propagator of  $\phi_A$  and a dashed line to that of  $\phi_B$ . A shaded blob is a vertex function, see Appendix A for the definition. It is assumed that  $\phi_A$  carries a conserved charge.

### 2.1 Boson mass shift formula in the $\phi_A$ - $\phi_B$ system

As the finite and infinite volume masses  $M_A(L)$ ,  $m_A$  of  $A$ -particle are defined from the poles of the propagators of  $\phi_A$  (see Appendix A),  $\Delta m_A(L) = M_A(L) - m_A$  is reduced to

$$\Delta m_A(L) = -\frac{1}{2m_A} [\Sigma_L(p) - \Sigma(p)] + O((\Delta m_A)^2) \quad \text{at } p = (im_A, \vec{0}), \quad (5)$$

where  $\Sigma_L(p)$  and  $\Sigma(p)$  stand for the self energies of  $\phi_A$  in the finite and infinite volumes, respectively. We work in Euclidean space as in Ref. [10]. Here, since the fermion mass shift formula in the fermion-boson system is of our final interest, we assume that only  $\phi_A$  carries a conserved charge so that interaction induced only by the 3-point vertex  $AAB$  and 4-point charge conserving vertices are taken into account. In such a system, the difference of the self energy of  $\phi_A$  in the finite and infinite volumes at any orders in perturbation theory is provided by the diagrams listed in Fig. 1. For  $m_B/m_A \in (0, 1]$ , Eq. (5) is reduced to

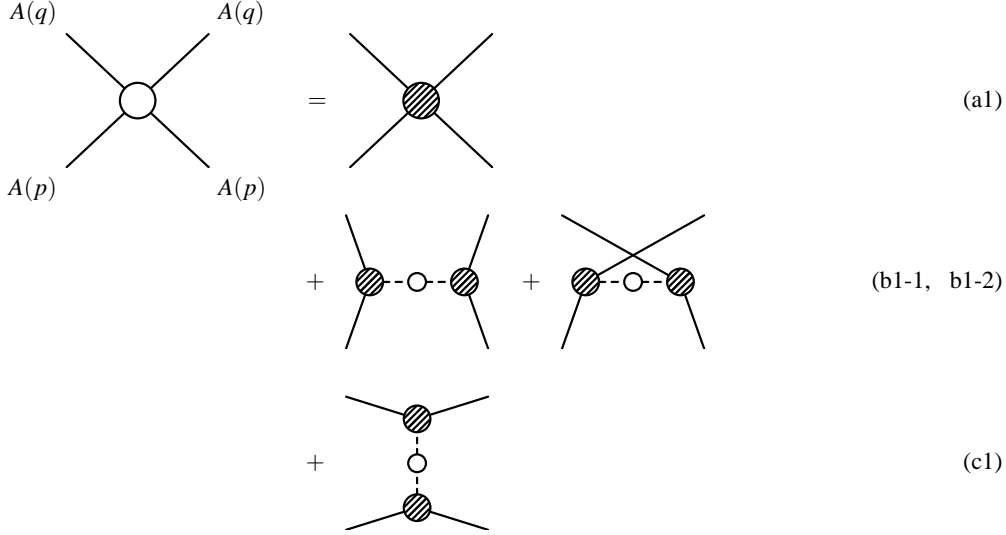


Fig. 2. Ingredients of  $F_{AA}(\nu)$  in the  $\phi_A$ - $\phi_B$  system. The labels represent the correspondence with the self-energy diagrams in Fig. 1. The diagram (b1) in Fig. 1 is responsible for the two types of amplitudes.

$$\Delta m_A(L) = -\frac{3}{8\pi m_A L} \left[ \frac{\lambda_{AAB}^2}{2\nu_B} e^{-L\sqrt{m_B^2 - \nu_B^2}} + \int_{-\infty}^{\infty} \frac{dq_0}{2\pi} e^{-L\sqrt{q_0^2 + m_A^2}} F_{AA}(iq_0) \right. \\ \left. + \int_{-\infty}^{\infty} \frac{dq_0}{2\pi} e^{-L\sqrt{q_0^2 + m_B^2}} F_{AB}(iq_0) \right] + O(e^{-L\bar{m}}), \quad (6)$$

where  $F_{AB}(\nu)$  and  $F_{AA}(\nu)$  denote the forward scattering amplitudes of the processes  $\phi_A(p) + \phi_B(q) \rightarrow \phi_A(p) + \phi_B(q)$  and  $\phi_A(p) + \phi_A(q) \rightarrow \phi_A(p) + \phi_A(q)$  in the infinite volume, respectively. The ingredients of these scattering amplitudes are graphically represented in Figs. 2 and 3.  $\lambda_{AAB}$  is an effective renormalized coupling defined from the residue of  $F_{AB}(\nu)$  at  $\nu = \pm\nu_B = \pm m_B^2/2m_A$  as

$$\lim_{\nu \rightarrow \pm\nu_B} (\nu^2 - \nu_B^2) F_{AB}(\nu) = \frac{\lambda_{AAB}^2}{2}. \quad (7)$$

The pole term in Eq. (6) is associated with the evaluation of the self-energy diagram (b1) in Fig. 1. The error term is defined by

$$\bar{m} \geq \sqrt{2(m_B^2 - \nu_B^2)}, \quad (8)$$

which is due to the neglect of  $|\bar{m}| \geq \sqrt{2}$  contributions. If  $m_B/m_A < \alpha_c = \sqrt{2 - \sqrt{2}} \approx 0.765$ , we may neglect the second term in Eq. (6), which decays more rapidly than the error term at large  $L$ . Note that the pole term in Eq. (6) is twice larger than that in Eq. (3) and two types of forward scattering

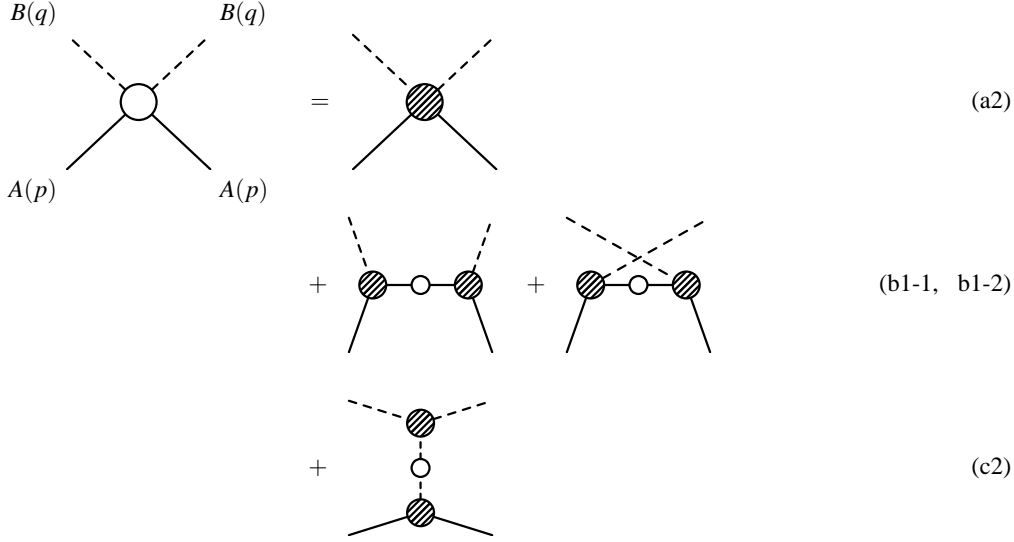


Fig. 3. Ingredients of  $F_{AB}(\nu)$  in the  $\phi_A$ - $\phi_B$  system (or in the  $\Psi_A$ - $\phi_B$  system with arrows to the solid lines). The labels represent the correspondence with the self-energy diagrams in Fig. 1.

amplitudes contribute to the formula in Eq. (6).

## 2.2 Fermion mass shift formula in the $\Psi_A$ - $\phi_B$ system

From the poles of the propagators of  $\Psi_A$  in the finite and infinite volumes (see Appendix A), we obtain

$$\Delta m_A = -\frac{1}{2m_A} \bar{u}(p, r) [\Sigma_L(p) - \Sigma(p)] u(p, r) + O((\Delta m_A)^2) \text{ at } p = (im_A, \vec{0}), \quad (9)$$

where  $\bar{u}(p, r)$  and  $u(p, r)$  are spinors of  $\Psi_A$  with the spin  $r$ . The mass shift is then written down as

$$\begin{aligned} \Delta m_A(L) = & -\frac{3}{8\pi m_A L} \left[ \frac{\lambda_{AAB}^2}{2\nu_B} e^{-L\sqrt{m_B^2 - \nu_B^2}} \right. \\ & - \int_{-\infty}^{\infty} \frac{dq_0}{2\pi} e^{-L\sqrt{q_0^2 + m_A^2}} \{F_{AA}(iq_0) + F_{A\bar{A}}(iq_0)\} \\ & \left. + \int_{-\infty}^{\infty} \frac{dq_0}{2\pi} e^{-L\sqrt{q_0^2 + m_B^2}} F_{AB}(iq_0) \right] + O(e^{-L\bar{m}}), \quad (10) \end{aligned}$$

where  $\bar{m}$  is the same as in Eq. (8). Now, three types of the forward scattering amplitudes contribute to the formula,  $F_{AB}(\nu)$ :  $\Psi_A(p) + \phi_B(q) \rightarrow \Psi_A(p) + \phi_B(q)$  (Compton type),  $F_{AA}(\nu)$ :  $\Psi_A(p) + \Psi_A(q) \rightarrow \Psi_A(p) + \Psi_A(q)$  (Møller type), and

$$\begin{aligned}
\Sigma_L(p) - \Sigma(p) = & \text{[Diagram: solid arrow with empty circle loop and shaded blob]} + \frac{1}{2} \left( \text{[Diagram: dashed arrow with empty circle loop and shaded blob]} \right) & \text{(a1, a2)} \\
& + \text{[Diagram: dashed arrow with empty circle loop and two shaded blobs]} & \text{(b1)} \\
& + \text{[Diagram: solid arrow with empty circle loop and shaded blob]} + \frac{1}{2} \left( \text{[Diagram: dashed arrow with empty circle loop and shaded blob]} \right) & \text{(c1, c2)}
\end{aligned}$$

Fig. 4. Self-energy diagrams which contribute to the mass shift formula in the  $\Psi_A$ - $\phi_B$  system. A solid arrow with an empty circle corresponds to the propagator of  $\Psi_A$ .

$$\begin{aligned}
& \text{[Diagram: vertex with four external lines labeled } A(q) \text{ and } A(p)] = \text{[Diagram: shaded blob vertex]} & \text{(a1)} \\
& + \text{[Diagram: vertex with four external lines and two shaded blobs]} + \text{[Diagram: vertex with four external lines and two shaded blobs]} & \text{(b1, c1)}
\end{aligned}$$

Fig. 5. Ingredients of  $F_{AA}(\nu)$  in the  $\Psi_A$ - $\phi_B$  system. The labels represent the correspondence with the self-energy diagrams in Fig. 4.

$F_{A\bar{A}}(\nu)$ :  $\Psi_A(p) + \bar{\Psi}_A(q) \rightarrow \Psi_A(p) + \bar{\Psi}_A(q)$  (Bhabha type) (see, Figs. 3, 5 and 6). Again we may neglect the second term if  $m_B/m_A < \alpha_c$ . Apart from the relative minus sign in front of the second term, which is due to Fermi statistics, the formula is almost the same as for the boson. The factor of the pole term is twice larger than that in Eq. (3).

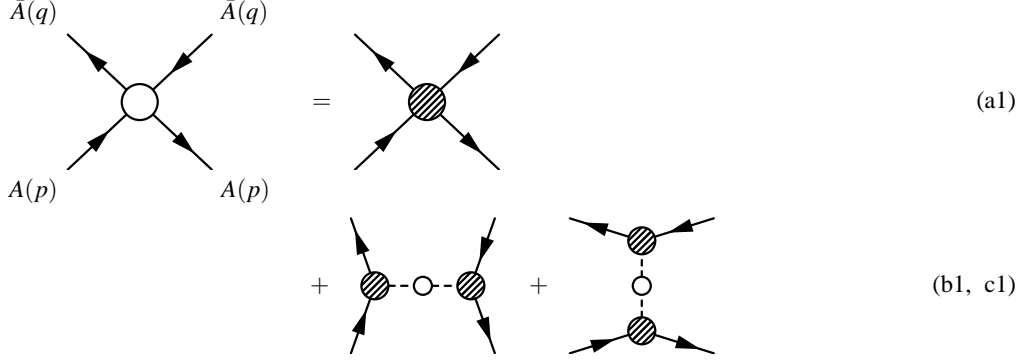


Fig. 6. Ingredients of  $F_{A\bar{A}}(\nu)$  in the  $\Psi_A\text{-}\phi_B$  system. The labels represent the correspondence with the self-energy diagrams in Fig. 4.

### 3 Outline of derivation

In this section, we provide a part of the derivation of the mass shift formulae in Eqs. (6) and (10) for the case

$$\alpha \equiv \frac{m_B}{m_A} \in (0, 1] . \quad (11)$$

We shall here concentrate on the evaluation of the self-energy diagram (b1) in Figs. 1 and 4, which is typical in the two particle system and finally provides the pole term  $O(e^{-L\mu})$  with

$$\mu \equiv m_B \sqrt{1 - \frac{\alpha^2}{4}} = \sqrt{m_B^2 - \nu_B^2} , \quad \nu_B = \frac{m_B^2}{2m_A} . \quad (12)$$

The definitions of the propagators and the vertex functions used in the following calculations are summarized in Appendix A. Other self-energy diagrams can be evaluated in a similar way. The results are collected in Appendix B.

#### 3.1 Boson mass shift formula

The self-energy diagram (b1) in Fig. 1 with  $|\vec{m}| = 1$  (see Eq. (4)) is given by

$$I_{b1} = \int \frac{d^4q}{(2\pi)^4} \left( 2 \sum_{j=1}^3 \cos Lq_j \right) \Gamma_{AAB}(-p, (1-\delta)p+q; \delta p-q) G_A((1-\delta)p+q) \\ \times G_B(\delta p-q) \Gamma_{AAB}(p, -(1-\delta)p-q; -\delta p+q) \Big|_{p=(im_A, \vec{0})} , \quad (13)$$



where  $\delta \in (0, \frac{1}{2}]$  is a parameter chosen optimally below. We are working in Euclidean space so that  $q_\mu = q^\mu = (q_0, \vec{q})$  and  $\vec{q} = (q_1, q_2, q_3)$ . Inner product is defined by  $pq = p_0q_0 + \vec{p} \cdot \vec{q} = im_A q_0$ . Due to rotational invariance among  $q_1, q_2$  and  $q_3$  one can rewrite the cosine factor in Eq. (13) as  $2 \sum_{j=1}^3 \cos Lq_j \rightarrow 6 \operatorname{Re} e^{iLq_1}$ .

Firstly, we integrate out  $q_1$ . To do this, we extend  $q_1$  to a complex variable and perform complex contour integration. Here, the integral path must be chosen appropriately by considering the analyticity properties of the integrand, the vertex functions and the propagators, in the complex  $q_1$  plane.

A complex domain  $\mathbb{D} = \{(p, q) \in \mathbb{C}^4 \times \mathbb{C}^4\}$ , to which the vertex function  $\Gamma_{AAB}(\mp p, \pm(1 - \delta)p \pm q; \pm\delta p \mp q)$  initially defined for  $(p, q) \in \mathbb{R}^4 \times \mathbb{R}^4$  is analytically extended, can be found as follows. The basic assumption here is that the vertex function at any orders in perturbation theory consists of a set of  $A$  and  $B$  lines (free propagators). The  $l$ -th  $A$  or  $B$  line is then parametrized as  $[(k(l) + r(l))^2 + m_A^2]^{-1}$  or  $[(k(l) + r(l))^2 + m_B^2]^{-1}$ , where  $k(l)$  is the flow of external momentum given by a combination of complex variables  $p$  and  $q$ , and  $r(l)$  is a combination of internal loop momenta to be integrated out, which is a real variable in Euclidean space. Thus, we find that the vertex function has no singularity if  $(\operatorname{Im} k(l))^2 < m_A^2$  and  $(\operatorname{Im} k(l))^2 < m_B^2$  are satisfied for all  $A$  and  $B$  lines. In order to find the possible choices of  $k(l)$ , we label the three bare vertices where the external momenta,  $\mp p, \pm(1 - \delta)p \pm q$  and  $\pm\delta p \mp q$ , are plugged in as  $a_1, a_2$  and  $b$ , respectively (e.g.  $a_1 = a_2 = b$  at the tree level). We consider here the case that  $A$ -particle carries a conserved charge. In this case, there always exists a set of  $A$  lines connecting  $a_1$  and  $a_2$ . We can then choose  $k(l)$  up to overall sign as follows. If the connected  $A$  lines flow through  $b$ , such  $A$  lines carry  $(1 - \delta)p - \frac{1}{2}q$  between  $a_1$  and  $b$ , and  $(1 - 2\delta)p + \frac{1}{2}q$  between  $b$  and  $a_2$ . The other lines then carry  $\delta p + \frac{1}{2}q$  or 0. If the connected  $A$  lines do not flow through  $b$ ,  $A$  lines carry  $(1 - \delta)p + \frac{1}{2}q$  between  $a_1$  and  $a_2$ , and the other lines carry  $\delta p, \frac{1}{2}q, \delta p - \frac{1}{2}q$  or 0. The analytic complex domain  $\mathbb{D}$  is then specified by inserting these  $k(l)$  into the above two inequalities. Practically, it is enough to consider the cases

$$\left(\operatorname{Im}\left\{(1 - \delta)p \pm \frac{1}{2}q\right\}\right)^2 < m_A^2, \quad (14)$$

$$\left(\operatorname{Im}\left\{\delta p \pm \frac{1}{2}q\right\}\right)^2 < m_B^2, \quad (15)$$

so that all other cases are fulfilled. <sup>2</sup> Solving these inequalities with  $\operatorname{Im} p_0 =$

<sup>2</sup> In a similar way, one can discuss the analyticity properties of  $\Gamma_{AAB}$  for the case neither  $\phi_A$  nor  $\phi_B$  carry the conserved charge. In this case, the coupling  $ABB$  can be present and therefore the r.h.s. of inequality (14) must be replaced by  $m_B^2$  for  $\alpha < 1$ . Then,  $\delta = 1/2$  will be an optimal choice, which provides the analytic

$m_A, \vec{p} = \vec{0}$ , and  $(q_0, q_\perp) \in \mathbb{R}^3$ , where  $q_\perp = (q_2, q_3)$ , we find that the choice

$$\delta = \frac{\alpha^2}{2} \quad (16)$$

provides a maximum analytic strip of  $\text{Im } q_1$ , in which the vertex function has no singularity:

$$0 \leq \text{Im } q_1 < 2m_B \sqrt{1 - \frac{\alpha^2}{4}} = 2\mu. \quad (17)$$

It is useful to find that if  $\alpha = 1$  ( $m_A = m_B \equiv m$ ), the parametrization of external momenta ( $\delta = 1/2$ ) and the analytic strip of  $\text{Im } q_1$  (maximum value is  $\sqrt{3}m$ ) are reduced to the case as discussed in Ref. [10] for the identical bosonic system.

Inserting Eq. (16) to the propagators  $G_A$  and  $G_B$  in Eq. (13), we find that these propagators possess poles of one-particle states at

$$q_1^{(A)} = i\sqrt{q_0^2 + q_\perp^2 + \mu^2 + i(2 - \alpha^2)m_A q_0}, \quad (18)$$

$$q_1^{(B)} = i\sqrt{q_0^2 + q_\perp^2 + \mu^2 - i\alpha m_B q_0}, \quad (19)$$

in the complex  $q_1$  upper half plane, respectively.<sup>3</sup> Note that these two poles happen to degenerate for  $q_0 = 0$  as

$$q_1^{(A)} = q_1^{(B)} = i\sqrt{q_\perp^2 + \mu^2}. \quad (22)$$

To avoid the double pole in the complex  $q_1$  plane, we may deform the  $q_0$  integration path around  $q_0 = 0$  into an infinitesimal half circle in the complex lower half plane (see Figs 7 and 8). For the purpose of controlling the error term associated with integration up to  $O(e^{-L\bar{m}})$  (with  $\bar{m} = \sqrt{2}\mu$ ), we consider  $q_0$  and  $q_\perp$  in the ball

strip  $0 \leq \text{Im } q_1 < 2m_B \sqrt{1 - 1/(4\alpha^2)}$ . Clearly this strip can be defined only for  $\alpha \in (1/2, 1]$ .

<sup>3</sup> For  $a, b \in \mathbb{R}$ ,

$$q \equiv i\sqrt{a + ib} = -\sqrt{(\sqrt{a^2 + b^2} - a)/2} + i\sqrt{(\sqrt{a^2 + b^2} + a)/2} \quad \text{if } b \geq 0, \quad (20)$$

$$= +\sqrt{(\sqrt{a^2 + b^2} - a)/2} + i\sqrt{(\sqrt{a^2 + b^2} + a)/2} \quad \text{if } b < 0. \quad (21)$$

$$\mathbb{B} = \{(q_0, q_\perp) \in \mathbb{R}^3 \mid q_0^2 + q_\perp^2 \leq \mu^2\}. \quad (23)$$

In this ball it turns out that  $\text{Im } q_1^{(A)}$  and  $\text{Im } q_1^{(B)}$  are inside the strips

$$m_B \sqrt{1 - \frac{\alpha^2}{4}} \leq \text{Im } q_1^{(A)} \leq m_B \sqrt{\frac{1}{\alpha} \sqrt{1 - \frac{\alpha^2}{4}} + 1 - \frac{\alpha^2}{4}}, \quad (24)$$

$$m_B \sqrt{1 - \frac{\alpha^2}{4}} \leq \text{Im } q_1^{(B)} \leq m_B \sqrt{\sqrt{1 - \frac{\alpha^2}{4}} + 1 - \frac{\alpha^2}{4}}, \quad (25)$$

respectively.

Now, we choose a contour depending on  $\alpha$ . If  $\alpha \in [\alpha_c, 1]$ , where  $\alpha_c \equiv \sqrt{2 - \sqrt{2}} \approx 0.765$ , we take a path which goes along the real  $q_1$  line and the line  $\text{Im } q_1 = \sqrt{\mu^2 + m_A^2}$  closed at  $\pm\infty$ . In this case, both  $q_1^{(A)}$  and  $q_1^{(B)}$  are completely inside the contour. If  $\alpha \in (0, \alpha_c)$ , we take the line  $\text{Im } q_1 = \sqrt{\mu^2 + m_B^2}$  instead of  $\sqrt{\mu^2 + m_A^2}$ . In this case, while  $q_1^{(B)}$  is completely inside the contour,  $q_1^{(A)}$  locates partially outside the contour. However, since even the lower bound of  $\text{Im } q_1^{(A)}$  exceeds  $\bar{m}$  for  $\alpha < \alpha_c$  at next step of the complex contour integration of  $q_0$ , we may neglect the  $q_1^{(A)}$  contribution here. In both cases the contribution from the path where  $\text{Im } q_1 \neq 0$  is negligible, since it is more rapidly decaying at large  $L$  than the error term  $O(e^{-L\bar{m}})$ . Then, from the residues at  $q_1^{(A)}$  and  $q_1^{(B)}$ , we obtain

$$I_{b1} = I_{b1}^{(A)} + I_{b1}^{(B)} + O(e^{-L\bar{m}}), \quad (26)$$

where

$$I_{b1}^{(A)} = 6i \int_{\mathbb{B}} \frac{dq_0 d^2 q_\perp}{(2\pi)^3} \frac{e^{iLq_1}}{2q_1} \Gamma_{AAB}(-p, (1-\delta)p+q; \delta p-q) G_B(\delta p-q) \\ \times \Gamma_{AAB}(p, -(1-\delta)p-q; -\delta p+q) \Big|_{q_1=q_1^{(A)}}, \quad (27)$$

$$I_{b1}^{(B)} = 6i \int_{\mathbb{B}} \frac{dq_0 d^2 q_\perp}{(2\pi)^3} \frac{e^{iLq_1}}{2q_1} \Gamma_{AAB}(-p, (1-\delta)p+q; \delta p-q) \\ \times G_A((1-\delta)p+q) \Gamma_{AAB}(p, -(1-\delta)p-q; -\delta p+q) \Big|_{q_1=q_1^{(B)}}. \quad (28)$$

As mentioned above,  $I_{b1}^{(A)}$  is relevant only for the case  $\alpha \in [\alpha_c, 1]$ . Note that  $G_B(\delta p-q) \Big|_{q_1=q_1^{(A)}}$  and  $G_A((1-\delta)p+q) \Big|_{q_1=q_1^{(B)}}$  have a common pole at  $q_0 = 0$ .

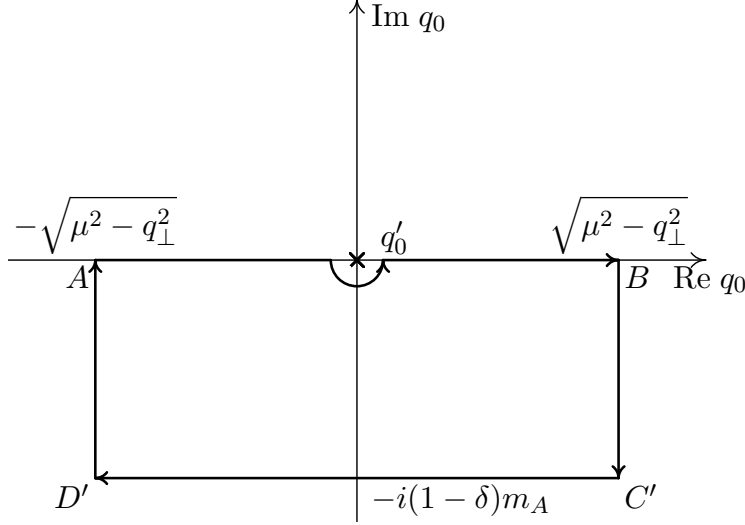


Fig. 7.  $q_0$  integral contour for  $I_{b1}^{(A)}$ .

Secondly, we perform the complex contour integration of  $q_0$ .  $I_{b1}^{(A)}$  is evaluated along the contour in Fig. 7. The contributions from the paths  $BC'$  and  $D'A$  are negligible at large  $L$ , since  $\text{Im } q_1^{(A)} \geq \bar{m}$  along these lines. The choice of the contour  $C'D'$  (given by the shift  $q_0 \rightarrow q_0 - i(1-\delta)m_A$ ) is possible because both inequalities (14) and (15) are satisfied as long as  $\alpha > \sqrt{3 - \sqrt{7}} \approx 0.595$  and thus the vertex function has no singularity inside the contour for  $\alpha \in [\alpha_c, 1]$ . As there is no pole inside the contour, the integral can be written as that along the path  $C'D'$ . The argument of the propagator  $G_B$  and  $q_1^{(A)}$  are then shifted as  $\delta p - q \rightarrow p - q$  and  $q_1^{(A)} \rightarrow i\sqrt{q_0^2 + q_\perp^2 + m_A^2}$ , respectively, where  $q$  satisfies the on-shell condition  $q^2 = -m_A^2$ . The integral is then represented as

$$I_{b1}^{(A)} = 6 \int_{\mathbb{B}} \frac{dq_0 d^2 q_\perp}{(2\pi)^3} \frac{e^{-L\sqrt{q_0^2 + q_\perp^2 + m_A^2}}}{2\sqrt{q_0^2 + q_\perp^2 + m_A^2}} F_{AA}^{(b1-2)}(iq_0) + O(e^{-L\bar{m}}), \quad (29)$$

where

$$F_{AA}^{(b1-2)}(iq_0) = \Gamma_{AAB}(-p, q; p - q) G_B(p - q) \times \Gamma_{AAB}(p, -q; -p + q)|_{p^2=q^2=-m_A^2} \quad (30)$$

is a one-particle-irreducible (1PI) part of the forward scattering amplitude of  $F_{AA}(\nu)$  with  $\nu = pq/m_A = iq_0$  (see the diagram (b1-2) in Fig. 2).

$I_{b1}^{(B)}$  is then evaluated along the contour in Fig. 8. Again the contributions from the paths  $BC$  and  $DA$  are negligible at large  $L$ , since  $\text{Im } q_1^{(B)} \geq \bar{m}$  along these lines. The integral along the path  $CD$  is parametrized by shifting the momentum as  $q_0 \rightarrow q_0 + i\delta m_A$ , which is possible because the vertex function

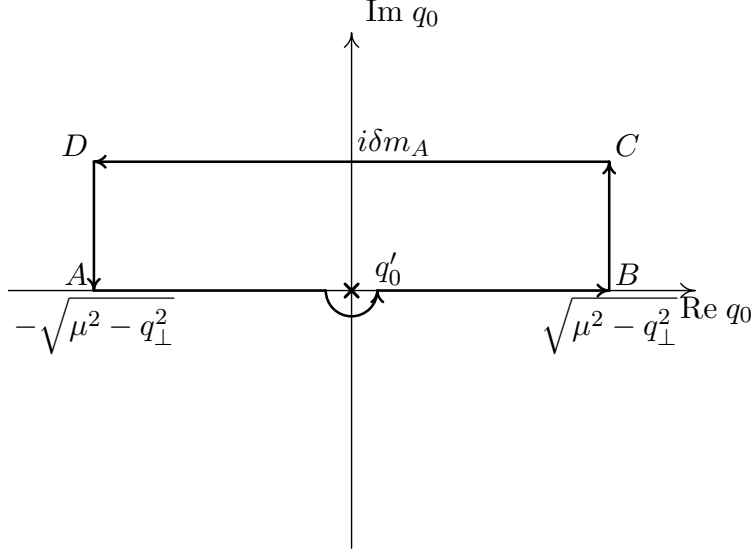


Fig. 8.  $q_0$  integral contour for  $I_{b1}^{(B)}$ .

is analytic inside the contour for the whole range of  $\alpha \in (0, 1]$ . The argument of  $G_A$  and  $q_1^{(B)}$  are shifted as  $(1 - \delta)p + q \rightarrow p + q$  and  $q_1^{(B)} \rightarrow i\sqrt{q_0^2 + q_\perp^2 + m_B^2}$  and then  $q^2 = -m_B^2$ . Now, since the pole at  $q_0 = 0$  is inside the contour, we also have a residue contribution. Thus the integral becomes

$$\begin{aligned}
I_{b1}^{(B)} &= 3 \int_{\mathbb{B}'} \frac{d^2 q_\perp}{(2\pi)^2} \frac{e^{-L\sqrt{q_\perp^2 + \mu^2}}}{2\sqrt{q_\perp^2 + \mu^2}} \frac{\lambda_{AAB}^2}{2\nu_B} \\
&+ 6 \int_{\mathbb{B}} \frac{dq_0 d^2 q_\perp}{(2\pi)^3} \frac{e^{-L\sqrt{q_0^2 + q_\perp^2 + m_B^2}}}{2\sqrt{q_0^2 + q_\perp^2 + m_B^2}} F_{AB}^{(b1-1)}(iq_0) + O(e^{-L\bar{m}}), \quad (31)
\end{aligned}$$

where

$$\begin{aligned}
F_{AB}^{(b1-1)}(iq_0) &= \Gamma_{AAB}(-p, p + q; -q) G_A(p + q) \\
&\times \Gamma_{AAB}(p, -p - q; q)|_{p^2 = -m_A^2, q^2 = -m_B^2} \quad (32)
\end{aligned}$$

is a 1PI part of the forward scattering amplitudes of  $F_{AB}(\nu)$  (see the diagram (b1-1) in Fig. 3). Note that  $F_{AB}^{(b1-1)}(\nu)$  has a pole at  $\nu = +\nu_B$ . The coupling  $\lambda_{AAB}$  in the first term in Eq. (31) is the effective renormalized coupling defined through the relation

$$\begin{aligned}
\frac{\lambda_{AAB}^2}{2} &= \lim_{\nu \rightarrow \pm\nu_B} (\nu^2 - \nu_B^2) F_{AB}(\nu) = \lim_{\nu \rightarrow +\nu_B} (\nu^2 - \nu_B^2) F_{AB}^{(b1-1)}(\nu) \\
&= \frac{\nu_B}{m_A} \Gamma_{AAB}(-p, p + q; -q) \Gamma_{AAB}(p, -p - q; q)|_{\nu = +\nu_B}, \quad (33)
\end{aligned}$$

where all legs of the vertex function is on the mass shell,  $p^2 = -m_A^2$ ,  $(p+q)^2 = -m_A^2$  and  $q^2 = -m_B^2$ . The integral region of  $q_\perp$  in the first term in Eq. (31) is defined by

$$\mathbb{B}' = \{q_\perp \in \mathbb{R}^2 \mid q_\perp^2 \leq \mu^2\}. \quad (34)$$

One may find that the 1PI amplitudes corresponding to (b1-1) in Fig. 2 and (b1-2) in Fig. 3, which are necessary to build up the forward scattering amplitudes in the mass shift formula, are apparently absent in  $I_{b1}$ . However, we find that these amplitudes can be included by using the crossing relation  $F_{AA}^{(b1-1)}(-\nu) = F_{AA}^{(b1-2)}(\nu)$  and  $F_{AB}^{(b1-1)}(-\nu) = F_{AB}^{(b1-2)}(\nu)$ ; one can replace  $F_{AA}^{(b1-2)}(\nu)$  in Eq. (29) by  $(F_{AA}^{(b1-1)}(\nu) + F_{AA}^{(b1-2)}(\nu))/2$  and  $F_{AB}^{(b1-1)}(\nu)$  in Eq. (31) by  $(F_{AB}^{(b1-1)}(\nu) + F_{AB}^{(b1-2)}(\nu))/2$ .

Finally, we carry out the  $q_\perp$  integration in Eqs. (29) and (31) using the formula

$$\int_{-\infty}^{\infty} \frac{d^2 q_\perp}{(2\pi)^2} \frac{e^{-L\sqrt{q_\perp^2 + \rho^2}}}{2\sqrt{q_\perp^2 + \rho^2}} = \frac{1}{4\pi L} e^{-L\rho}, \quad (35)$$

where the integral region is extended from  $\mathbb{B}$  or  $\mathbb{B}'$  to the infinity, because the additional contributions are always up to the order of the error term. Hence, we end up with

$$\begin{aligned} I_{b1} = & \frac{3}{4\pi L} \left[ \frac{\lambda_{AAB}^2}{2\nu_B} e^{-L\mu} \right. \\ & + \int_{-\infty}^{\infty} \frac{dq_0}{2\pi} e^{-L\sqrt{q_0^2 + m_A^2}} \{F_{AA}^{(b1-1)}(iq_0) + F_{AA}^{(b1-2)}(iq_0)\} \\ & \left. + \int_{-\infty}^{\infty} \frac{dq_0}{2\pi} e^{-L\sqrt{q_0^2 + m_B^2}} \{F_{AB}^{(b1-1)}(iq_0) + F_{AB}^{(b1-2)}(iq_0)\} \right] + O(e^{-L\bar{m}}). \quad (36) \end{aligned}$$

By combining the contributions from the other self-energy diagrams in Fig. 1 (see Appendix B), we complete Eq. (6).

### 3.2 Fermion mass shift formula

Let us next consider the fermion mass shift formula in the  $\Psi_A\text{-}\phi_B$  system. The self-energy diagram (b1) in Fig. 4 with  $|\vec{m}| = 1$ , sandwiched by the spinors  $\bar{u}(p, r)$  and  $u(p, r)$ , is given by

$$\begin{aligned}
I_{b1} = & \int \frac{d^4 q}{(2\pi)^4} \left( 2 \sum_{j=1}^3 \cos Lq_j \right) \bar{u}(p, r) \Gamma_{AAB}(-p, (1-\delta)p+q; \delta p-q) \\
& \times S_A((1-\delta)p+q) G_B(\delta p-q) \Gamma_{AAB}(p, -(1-\delta)p-q; -\delta p+q) \\
& \times u(p, r) \Big|_{p=(im_A, \vec{0})}. \tag{37}
\end{aligned}$$

Since the pole structure of the integrand is the same as in the  $\phi_A$ - $\phi_B$  system, we can carry out the momentum integration in a similar way.

After several integration steps, we then arrive at the expressions (see Figs. 5 and 3, respectively):

$$I_{b1}^{(A)} = -3 \int \frac{dq_0 d^2 q_\perp}{(2\pi)^3} \frac{e^{-L\sqrt{q_0^2+q_\perp^2+m_A^2}}}{2\sqrt{q_0^2+q_\perp^2+m_A^2}} \{F_{AA}^{(b1)}(iq_0) + F_{A\bar{A}}^{(b1)}(iq_0)\} + O(e^{-L\bar{m}}), \tag{38}$$

$$\begin{aligned}
F_{AA}^{(b1)}(iq_0) = & - \sum_s \bar{u}_\alpha(p, r) \Gamma_{AAB}^{\alpha\beta}(-p, q; p-q) u_\beta(q, s) G_B(p-q) \\
& \times \bar{u}_\gamma(q, s) \Gamma_{AAB}^{\gamma\delta}(p, -q; -p+q) u_\delta(p, r) \Big|_{p^2=q^2=-m_A^2}, \tag{39}
\end{aligned}$$

$$\begin{aligned}
F_{A\bar{A}}^{(b1)}(iq_0) = & \sum_s \bar{u}_\alpha(p, r) \Gamma_{AAB}^{\alpha\beta}(-p, -q; p+q) v_\beta(q, s) G_B(p+q) \\
& \times \bar{v}_\gamma(q, s) \Gamma_{AAB}^{\gamma\delta}(p, q; -p-q) u_\delta(p, r) \Big|_{p^2=q^2=-m_A^2}, \tag{40}
\end{aligned}$$

and

$$\begin{aligned}
I_{b1}^{(B)} = & 3 \int \frac{d^2 q_\perp}{(2\pi)^2} \frac{e^{-L\sqrt{q_\perp^2+\mu^2}}}{2\sqrt{q_\perp^2+\mu^2}} \frac{\lambda_{AAB}^2}{2\nu_B} \\
& + 3 \int \frac{dq_0 d^2 q_\perp}{(2\pi)^3} \frac{e^{-L\sqrt{q_0^2+q_\perp^2+m_B^2}}}{2\sqrt{q_0^2+q_\perp^2+m_B^2}} \{F_{AB}^{(b1-1)}(iq_0) + F_{AB}^{(b1-2)}(iq_0)\} + O(e^{-L\bar{m}}), \tag{41}
\end{aligned}$$

$$\begin{aligned}
F_{AB}^{(b1-1)}(iq_0) = & \bar{u}_\alpha(p, r) \Gamma_{AAB}^{\alpha\beta}(-p, p+q; -q) S_A^{\beta\gamma}(p+q) \\
& \times \Gamma_{AAB}^{\gamma\delta}(p, -p-q; q) u_\delta(p, r) \Big|_{p^2=-m_A^2, q^2=-m_B^2}, \tag{42}
\end{aligned}$$

$$\begin{aligned}
F_{AB}^{(b1-2)}(iq_0) = & \bar{u}_\alpha(p, r) \Gamma_{AAB}^{\alpha\beta}(-p, p-q; q) S_A^{\beta\gamma}(p-q) \\
& \times \Gamma_{AAB}^{\gamma\delta}(p, -p+q; -q) u_\delta(p, r) \Big|_{p^2=-m_A^2, q^2=-m_B^2}, \tag{43}
\end{aligned}$$

where we have used the relations  $m_A - i\cancel{q} = \sum_s u(q, s) \bar{u}(q, s)$  and  $m_A + i\cancel{q} = -\sum_s v(q, s) \bar{v}(q, s)$  in Eqs. (39) and (40), respectively. Repeated Greek letters, corresponding to spinor components, are implicitly summed. The overall minus sign in  $F_{AA}^{(b1)}$  is due to Fermi statistics. The effective coupling  $\lambda_{AAB}$  is defined as in Eq. (33). The advantage of such a definition of the coupling in the

fermion-boson system is that the model dependent matrix structure of the vertex function, such as  $\{I, \gamma_\mu, \sigma_{\mu\nu}, \gamma_5 \gamma_\mu, \gamma_5\}$ , is involved in  $\lambda_{AAB}$  through the definition of  $F_{AB}$ .

After integrating out  $q_\perp$ , we obtain the expression

$$I_{b1} = \frac{3}{4\pi L} \left[ \frac{\lambda_{AAB}^2}{2\nu_B} e^{-L\mu} - \int_{-\infty}^{\infty} \frac{dq_0}{2\pi} e^{-L\sqrt{q_0^2+m_A^2}} \{F_{AA}^{(b1)}(iq_0) + F_{A\bar{A}}^{(b1)}(iq_0)\} + \int_{-\infty}^{\infty} \frac{dq_0}{2\pi} e^{-L\sqrt{q_0^2+m_B^2}} \{F_{AB}^{(b1-1)}(iq_0) + F_{AB}^{(b1-2)}(iq_0)\} \right] + O(e^{-L\bar{m}}). \quad (44)$$

We find that the expression is almost equivalent to Eq. (36) apart from the relative minus sign in the second term. By combining the contribution from the other self-energy diagrams (see Appendix B), we complete Eq. (10).

#### 4 The nucleon mass shift

As an application of the fermion mass shift formula in Eq. (10), let us discuss the nucleon mass shift in the  $N$ - $\pi$  system. Since the formula is expected to hold nonperturbatively, it is interesting to estimate the mass shift by inserting the  $N$ - $\pi$  scattering amplitude which is known from experiment. Therefore, the following analysis can be regarded as an estimate of the finite volume effect on the nucleon mass when the realistic pion mass is achieved in lattice QCD simulations with dynamical fermions.

According to Höhler [12], the subthreshold expansion of the  $N$ - $\pi$  forward scattering amplitude around  $\nu = 0$  is parametrized as

$$F_{N\pi}(\nu) = 6m_N D^+(\nu), \quad (45)$$

where

$$D^+(\nu) = \frac{g^2}{m_N} \frac{\nu_B^2}{\nu_B^2 - \nu^2} + d_{00}^+ m_\pi^{-1} + d_{10}^+ m_\pi^{-3} \nu^2 + d_{20}^+ m_\pi^{-5} \nu^4 + O(\nu^6). \quad (46)$$

The isospin sum is taken in Eq. (45) and the effect of isospin symmetry breaking is neglected. The masses of the nucleon and pion are then given by  $m_N = 938$  MeV and  $m_\pi = 140$  MeV. The coupling constant is  $g^2/4\pi = 14.3$ . The first term in Eq. (46) is identified with the pseudovector nucleon Born



term with  $\nu_B = m_\pi^2/2m_N \approx 0.07m_\pi$ . The coefficients of the other terms are given by  $d_{00}^+ = -1.46(10)$ ,  $d_{10}^+ = 1.12(2)$  and  $d_{20}^+ = 0.200(5)$  [12]. We only take into account the mean of these values hereafter. Note that although Eq. (45) is defined in Minkowski space-time such that  $\nu$  is a real variable here, it can directly be inserted to Eq. (10) by rotating this variable as  $\nu = iq_0$ , where  $q_0$  is the integral variable in Eq. (10). The effective coupling is computed by using Eq. (7) as

$$\lim_{\nu \rightarrow \pm \nu_B} (\nu^2 - \nu_B^2) F_{N\pi}(\nu) = \frac{\lambda_{NN\pi}^2}{2} = -6g^2\nu_B^2. \quad (47)$$

Since  $m_\pi/m_N = 0.149 < \alpha_c$ , we may neglect the second term in Eq. (10). It is clear that since the factor of the pole term in Eq. (10) is already twice larger than that in Eq. (3), we obtain a different expression from that in Ref. [9]. In fact, the mass shift formula, divided by the nucleon mass itself, is reduced to

$$\begin{aligned} \delta(\xi = Lm_\pi) &\equiv \Delta m_N(L)/m_N \\ &= \frac{9}{2\xi} \left(\frac{g^2}{4\pi}\right) \left(\frac{m_\pi}{m_N}\right)^3 e^{-\xi\sqrt{1-\nu_B^2/m_\pi^2}} \\ &\quad - \frac{3}{16\pi^2\xi} \left(\frac{m_\pi}{m_N}\right)^2 \int_{-\infty}^{\infty} dy e^{-\xi\sqrt{1+y^2}} F_{N\pi}(im_\pi y) + O(e^{-L\bar{m}}) \\ &= \delta_P(\xi) + \delta_B(\xi) + \delta_R(\xi) + O(e^{-L\bar{m}}), \end{aligned} \quad (48)$$

where  $\delta_P(\xi)$  is the pole term, and  $\delta_B(\xi)$  and  $\delta_R(\xi)$  correspond to the contributions of the pseudovector Born term and the rest in Eq. (46). Clearly, this formula recovers the expression given in the framework of ChPT [6].

We plot  $\delta(\xi)$  in Fig. 9, where  $\xi = 1$  corresponds to  $L = 1.4$  fm. We find that  $\delta(\xi)$  suffers strongly from higher order contributions of  $\nu$  in the range  $\xi \leq 1$ . For instance,  $\delta_R(\xi)$  causes the negative mass shift within the leading mass shift formula ( $|\vec{m}| = 1$ ). In this range, the contribution from  $|\vec{m}| \geq \sqrt{2}$  to the formula, of course, will not be negligible. On the other hand,  $\delta(\xi)$  seems to be mostly described by  $\delta_P(\xi)$  as  $\xi$  increases. However we notice that this is due to the cancellation between  $\delta_B(\xi)$  and  $\delta_R(\xi)$ .

Finally, let us discuss the relation between the general fermion mass shift formula in Eq. (10) and the nucleon mass shift formula derived in Ref. [6]. The diagrams that they evaluated within ChPT correspond to (b1) and (a2) in Fig. 4, where the vertex functions were treated as certain coupling constants. The diagram (b1) was evaluated by introducing the Feynman parameter  $x$ , where its initial integral range  $x \in [0, 1]$  was modified as  $[0, 1] = (-\infty, \infty) - (-\infty, 0) - (1, \infty)$  and the terms of  $O(e^{-Lm_N})$  which mainly originate from the integral in the interval  $(1, \infty)$  were omitted according to the infrared regularization [1]. Then, from the integrals in the range  $(-\infty, \infty)$

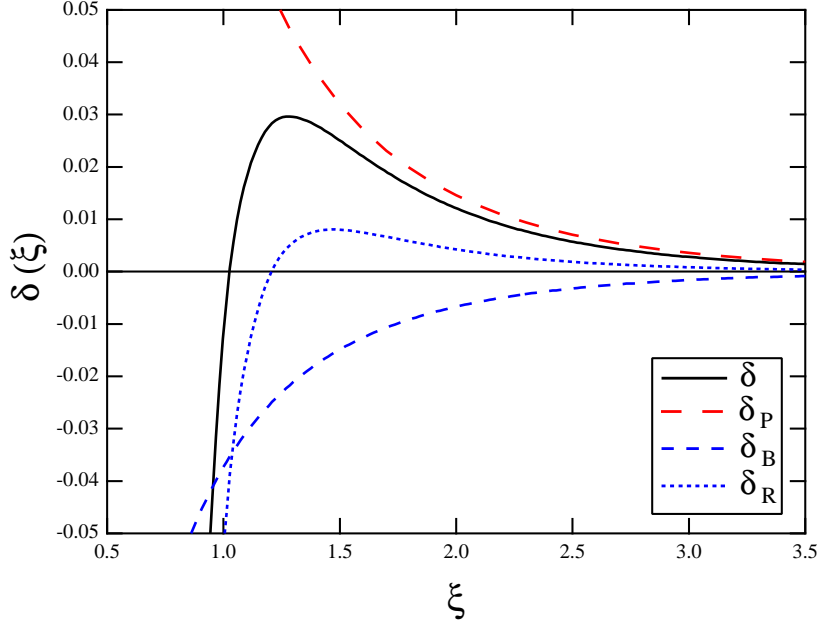


Fig. 9. The nucleon mass shift as a function of  $\xi = Lm_\pi$ .

and  $(-\infty, 0)$ , they obtained the terms corresponding to  $\delta_P(\xi)$  and  $\delta_B(\xi)$  in the mass shift formula, respectively. The evaluation of the diagram (a2) was straightforward and they obtained terms for  $\delta_R(\xi)$ . In our point of view this is reasonable since the diagram (a2) has nothing to do with the pole term. Here, it is interesting to notice that the omitted terms according to the infrared regularization can exactly be used to reconstruct the terms involving  $F_{NN}(\nu)$  and  $F_{N\bar{N}}(\nu)$ , which we have also omitted in Eq. (48) because of  $\alpha < \alpha_c$ . In this sense, the general formula in Eq. (10) covers all possible contributions to the mass shift, some of which may be neglected depending on the physical situation.

## 5 Summary

We have studied the general finite size mass shift formula for the two stable distinguishable particle system in a periodic finite volume along the lines of Lüscher's proof for an identical bosonic theory. The main results are Eqs. (6) and (10). What we have clarified are the following.

The boson mass shift formula for  $\phi_A$  in the  $\phi_A$ - $\phi_B$  system is related to *two* types of the forward scattering amplitudes,  $F_{AB}(\nu)$  and  $F_{AA}(\nu)$ . If  $m_B/m_A < \alpha_c = \sqrt{2 - \sqrt{2}} \approx 0.765$ , the contribution from the  $F_{AA}(\nu)$  term becomes smaller than the order of the error term. It has turned out that the speculation such as in Eq. (3) is not valid for a two particle system. However, the mechanism how the mass shift, proportional to the difference of the self energy  $\Sigma_L - \Sigma$ ,

is related to the forward scattering amplitude is the same as in the identical bosonic system [10]. In principle, the difference of the self energy consists of the propagators of  $\phi_A$  and  $\phi_B$ , one of which is broken into external legs on the mass shell after integration over the loop momentum. Then, a self-energy diagram is related to one (or some) of the 1PI parts of the forward scattering amplitude. It is to be noted that in the two particle system, unless the crossing symmetry among the 1PI parts of the amplitude is made manifest, some of the 1PI parts necessary to build up the forward scattering amplitudes will apparently be missed although such an expression is mathematically consistent. (In the identical particle system, the crossing symmetry is automatically manifest.)

The fermion mass shift formula for  $\Psi_A$  in the  $\Psi_A\text{-}\phi_B$  system is related to *three* types of the forward scattering amplitudes,  $F_{AB}(\nu)$ ,  $F_{AA}(\nu)$  and  $F_{A\bar{A}}(\nu)$ . If  $m_B/m_A < \alpha_c$ , the contributions from the  $F_{AA}(\nu)$  and  $F_{A\bar{A}}(\nu)$  terms become smaller than the order of the error term. Again, crossing symmetry must be taken into account to relate the self-energy diagrams to all 1PI parts of the forward scattering amplitudes. When the fermion propagator is broken into external legs on the mass shell, the relative minus sign appears in front of the corresponding terms.

In both cases,  $\lambda_{AAB} = 0$  unless the self energy contains the (b1) diagram, since it means that  $F_{AB}(\nu)$  has no pole.

Finally, we have written down the nucleon mass shift formula by applying the fermion mass shift formula in Eq. (10) to the  $N\text{-}\pi$  system, thereby we have found that the pole term is underestimated by factor two in Lüscher's formula in Ref. [9] and the formula derived in ChPT [6] is reproduced.

There are now general finite size mass shift formulae for the two particle systems which are valid to all orders in perturbation theory within  $|\vec{m}| = 1$ , in addition to that in the identical bosonic system [10]. For every case all these formulae are obtained in the same way by carefully analyzing the appropriate set of self-energy diagrams.

## Acknowledgments

We are grateful to P. Weisz for introducing us to this interesting topic and also for numerous discussions during the course of the present work. We also appreciate useful comments from M. Lüscher and G. Colangelo. We are partially supported by the DFG Forschergruppe 'Lattice Hadron Phenomenology.' M.K. is also supported by Alexander von Humboldt foundation, Germany.

## A Notation

In this appendix, we summarize our notations.

### A.1 Boson propagator

The boson propagator in infinite volume in Euclidean space is defined by

$$G(x-y) = \int \frac{d^4p}{(2\pi)^4} G(p) e^{ip(x-y)} , \quad (\text{A.1})$$

$$G(p) = \frac{1}{p^2 + m^2 - \Sigma(p)} , \quad (\text{A.2})$$

$$\Sigma(p) = \frac{\partial}{\partial p^2} \Sigma(p) = 0 \quad \text{for} \quad p^2 = -m^2 , \quad (\text{A.3})$$

where  $m$  is the physical mass. The renormalization conditions (A.3) mean that the propagator has pole at  $p^2 = -m^2$  with unit residue. We assume that there are no bound states so that this pole is the only singularity of  $G(p)$  below the two-particle threshold.

In the finite volume of the size  $L^3$ , by imposing periodic boundary conditions for the spatial directions, we have

$$G_L(x-y) = \frac{1}{L^3} \sum_{\vec{p}} \int \frac{dp_0}{2\pi} G_L(p) e^{ip(x-y)} , \quad (\text{A.4})$$

$$G_L(p) = \frac{1}{p^2 + m^2 - \Sigma_L(p)} , \quad (\text{A.5})$$

where the momenta are quantized as  $\vec{p} = 2\pi\vec{n}/L$  ( $\vec{n} \in \mathbb{Z}^3$ ). The summation of discrete momenta can be reformulated as the integral by using the Poisson summation formula (see Eq. (4)). We expect that the pole position of  $G_L(p)$  is shifted from  $p^2 = -m^2$  to  $p^2 = -M(L)^2$  with  $M(L) \equiv m + \Delta m(L)$ .

In the  $\phi_A$ - $\phi_B$  system, by expanding  $\Sigma_L(p)$  in powers of  $\Delta m_A(L)$ , we then solve

$$G_L(p)^{-1} \Big|_{p^2 = -M_A(L)^2} = 0 , \quad (\text{A.6})$$

and obtain Eq. (5) for  $\Delta m_A(L)$ .

## A.2 Fermion propagator

The fermion propagator in infinite volume in Euclidean space is

$$S(x-y) = \int \frac{d^4p}{(2\pi)^4} S(p) e^{ip(x-y)} , \quad (\text{A.7})$$

$$S(p) = \frac{1}{i\not{p} + m - \Sigma(p)} , \quad (\text{A.8})$$

$$\Sigma(p) = \frac{\partial}{\partial \not{p}} \Sigma(p) = 0 \quad \text{for} \quad i\not{p} = -m , \quad (\text{A.9})$$

where  $\not{p} \equiv \gamma_0^E p_0 + \gamma_i^E p_i$ . Euclidean Dirac matrices are defined by  $\gamma_0^E = \gamma_0$  and  $\gamma_i^E = i\gamma_i = -i\gamma^i$  ( $i = 1, 2, 3$ ), which satisfy  $\{\gamma_\mu^E, \gamma_\nu^E\} = 2\delta_{\mu\nu}$ . As similar to the boson propagator, we also assume that there are no bound states so that the pole at  $i\not{p} = -m$  is the only singularity of  $S(p)$  below the two-particle threshold.

In the finite volume of the size  $L^3$  with periodic boundary conditions, we have

$$S_L(x-y) = \frac{1}{L^3} \sum_{\vec{p}} \int \frac{dp_0}{2\pi} S_L(p) e^{ip(x-y)} , \quad (\text{A.10})$$

$$S_L(p) = \frac{1}{i\not{p} + m - \Sigma_L(p)} , \quad (\text{A.11})$$

where we expect that the pole position is shifted from  $i\not{p} = -m$  to  $i\not{p} = -M(L)$  with  $M(L) = m + \Delta m(L)$ .

In the  $\Psi_A$ - $\phi_B$  system, we then solve the equation

$$\bar{u}(p, r) S_L(p)^{-1} u(p, r)|_{p^2 = -M_A(L)^2} = 0 , \quad (\text{A.12})$$

where  $\bar{u}(p, r)$  and  $u(p, r)$  are spinors of  $\Psi_A$  defined as the solution of the free Dirac equation

$$\begin{aligned} (i\not{p} + m)u(p, r) &= 0 , & \bar{u}(p, r)(i\not{p} + m) &= 0 , \\ \bar{u}(p, r)u(p, s) &= 2m\delta_{rs} , \end{aligned} \quad (\text{A.13})$$

and obtain Eq. (9) for  $\Delta m_A(L)$ .

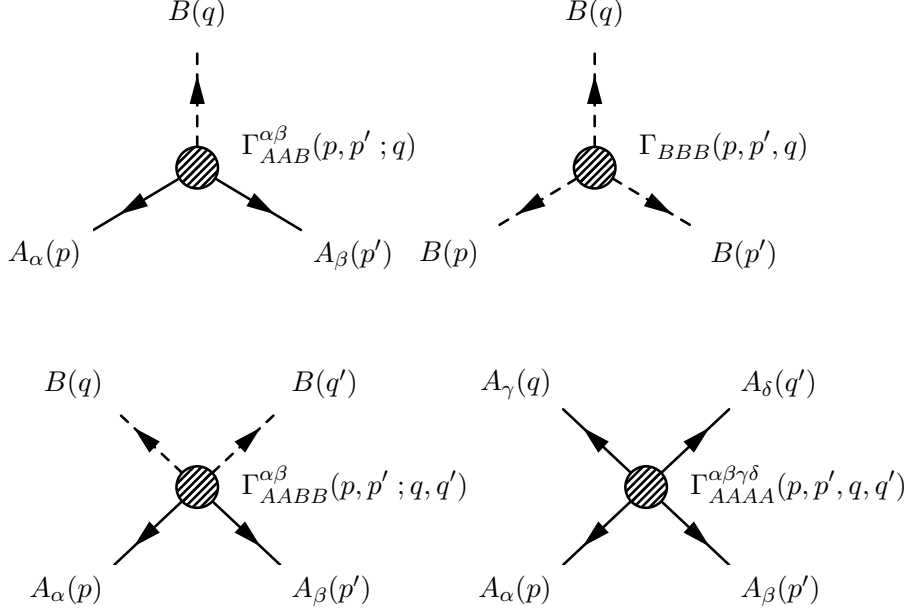


Fig. A.1. Vertex functions used in Figs. 1~6.

### A.3 Vertex functions

In Fig. A.1, we list all types of the vertex functions used in Figs. 1~6. Arrows represent the direction of momentum flow. Outgoing momenta from the vertex are parametrized to have positive sign. Greek letters denote spinor indices for the  $\Psi_A$ - $\phi_B$  system.

## B Ingredients of the formulae

We list all contributions to  $\Sigma_L(p) - \Sigma(p)$  in the  $\phi_A$ - $\phi_B$  system (Fig. 1) and  $\bar{u}(p, r)[\Sigma_L(p) - \Sigma(p)]u(p, r)$  in the  $\Psi_A$ - $\phi_B$  system (Fig. 4).

### B.1 $\phi_A$ - $\phi_B$ system

$$I_{a1} = \frac{3}{4\pi L} \int_{-\infty}^{\infty} \frac{dq_0}{2\pi} e^{-L\sqrt{q_0^2 + m_A^2}} F_{AA}^{(a1)}(iq_0) + O(e^{-L\bar{m}}), \quad (\text{B.1})$$

$$F_{AA}^{(a1)}(iq_0) \equiv \Gamma_{AAAA}(-p, p, -q, q)|_{p^2=q^2=-m_A^2},$$

$$I_{a2} = \frac{3}{4\pi L} \int_{-\infty}^{\infty} \frac{dq_0}{2\pi} e^{-L\sqrt{q_0^2 + m_B^2}} F_{AB}^{(a2)}(iq_0) + O(e^{-L\bar{m}}), \quad (\text{B.2})$$

$$F_{AB}^{(a2)}(iq_0) \equiv \Gamma_{AABB}(-p, p; -q, q)|_{p^2=-m_A^2, q^2=-m_B^2},$$

$$I_{b1} = \frac{3}{4\pi L} \left[ \frac{\lambda_{AAB}^2}{2\nu_B} e^{-L\sqrt{m_B^2-\nu_B^2}} \right. \\ \left. + \int_{-\infty}^{\infty} \frac{dq_0}{2\pi} e^{-L\sqrt{q_0^2+m_A^2}} \{F_{AA}^{(b1-1)}(iq_0) + F_{AA}^{(b1-2)}(iq_0)\} \right. \\ \left. + \int_{-\infty}^{\infty} \frac{dq_0}{2\pi} e^{-L\sqrt{q_0^2+m_B^2}} \{F_{AB}^{(b1-1)}(iq_0) + F_{AB}^{(b1-2)}(iq_0)\} \right] + O(e^{-L\bar{m}}), \quad (\text{B.3})$$

$$F_{AA}^{(b1-1)}(iq_0) \equiv \Gamma_{AAB}(-p, -q; p+q)G_B(p+q) \\ \times \Gamma_{AAB}(p, q; -p-q)|_{p^2=q^2=-m_A^2},$$

$$F_{AA}^{(b1-2)}(iq_0) \equiv \Gamma_{AAB}(-p, q; p-q)G_B(p-q) \\ \times \Gamma_{AAB}(p, -q; -p+q)|_{p^2=q^2=-m_A^2},$$

$$F_{AB}^{(b1-1)}(iq_0) \equiv \Gamma_{AAB}(-p, p+q; -q)G_A(p+q) \\ \times \Gamma_{AAB}(p, -p-q; q)|_{p^2=-m_A^2, q^2=-m_B^2},$$

$$F_{AB}^{(b1-2)}(iq_0) \equiv \Gamma_{AAB}(-p, p-q; q)G_A(p-q) \\ \times \Gamma_{AAB}(p, -p+q; -q)|_{p^2=-m_A^2, q^2=-m_B^2},$$

$$I_{c1} = \frac{3}{4\pi L} \int_{-\infty}^{\infty} \frac{dq_0}{2\pi} e^{-L\sqrt{q_0^2+m_A^2}} F_{AA}^{(c1)}(iq_0) + O(e^{-L\bar{m}}), \quad (\text{B.4})$$

$$F_{AA}^{(c1)}(iq_0) \equiv \Gamma_{AAB}(-p, p; 0)G_B(0)\Gamma_{AAB}(-q, q; 0)|_{p^2=q^2=-m_A^2},$$

$$I_{c2} = \frac{3}{4\pi L} \int_{-\infty}^{\infty} \frac{dq_0}{2\pi} e^{-L\sqrt{q_0^2+m_B^2}} F_{AB}^{(c2)}(iq_0) + O(e^{-L\bar{m}}), \quad (\text{B.5})$$

$$F_{AB}^{(c2)}(iq_0) \equiv \Gamma_{AAB}(-p, p; 0)G_B(0)\Gamma_{BBB}(0, -q, q)|_{p^2=-m_A^2, q^2=-m_B^2}.$$

The forward scattering amplitudes are defined by

$$F_{AA}(iq_0) = F_{AA}^{(a1)}(iq_0) + F_{AA}^{(b1-1)}(iq_0) + F_{AA}^{(b1-2)}(iq_0) + F_{AA}^{(c1)}(iq_0), \quad (\text{B.6})$$

$$F_{AB}(iq_0) = F_{AB}^{(a2)}(iq_0) + F_{AB}^{(b1-1)}(iq_0) + F_{AB}^{(b1-2)}(iq_0) + F_{AB}^{(c2)}(iq_0). \quad (\text{B.7})$$

## B.2 $\Psi_A\text{-}\phi_B$ system

$$I_{a1} = -\frac{3}{4\pi L} \int_{-\infty}^{\infty} \frac{dq_0}{2\pi} e^{-L\sqrt{q_0^2+m_A^2}} \{F_{AA}^{(a1)}(iq_0) + F_{AA}^{(a1)}(iq_0)\} + O(e^{-L\bar{m}}), \quad (\text{B.8})$$

$$F_{AA}^{(a1)}(iq_0) \equiv -\sum_s \bar{u}_\alpha(p, r)u_\beta(p, r)\bar{u}_\gamma(q, s)u_\delta(q, s) \\ \times \Gamma_{AAAA}^{\alpha\beta\gamma\delta}(-p, p, -q, q)|_{p^2=q^2=-m_A^2},$$

$$F_{AA}^{(a1)}(iq_0) \equiv \sum_s \bar{u}_\alpha(p, r) v_\beta(p, r) \bar{v}_\gamma(q, s) u_\delta(q, s) \\ \times \Gamma_{AAAA}^{\alpha\beta\gamma\delta}(-p, p, q, -q)|_{p^2=q^2=-m_A^2},$$

$$I_{a2} = \frac{3}{4\pi L} \int_{-\infty}^{\infty} \frac{dq_0}{2\pi} e^{-L\sqrt{q_0^2+m_B^2}} F_{AB}^{(a2)}(iq_0) + O(e^{-L\bar{m}}), \quad (\text{B.9}) \\ F_{AB}^{(a2)} \equiv \bar{u}_\alpha(p, r) \Gamma_{AABB}^{\alpha\beta}(-p, p; -q, q) u_\beta(p, r)|_{p^2=-m_A^2, q^2=-m_B^2},$$

$$I_{b1} = \frac{3}{4\pi L} \left[ \frac{\lambda_{AAB}^2}{2\nu_B} e^{-L\sqrt{m_B^2-\nu_B^2}} \right. \\ \left. - \int_{-\infty}^{\infty} \frac{dq_0}{2\pi} e^{-L\sqrt{q_0^2+m_A^2}} \{F_{AA}^{(b1)}(iq_0) + F_{AA}^{(b1)}(iq_0)\} \right. \\ \left. + \int_{-\infty}^{\infty} \frac{dq_0}{2\pi} e^{-L\sqrt{q_0^2+m_B^2}} \{F_{AB}^{(b1-1)}(iq_0) + F_{AB}^{(b1-2)}(iq_0)\} \right] + O(e^{-L\bar{m}}), \quad (\text{B.10})$$

$$F_{AA}^{(b1)}(iq_0) \equiv - \sum_s \bar{u}_\alpha(p, r) \Gamma_{AAB}^{\alpha\beta}(-p, -q; p+q) u_\beta(q, s) G_B(p+q) \\ \times \bar{u}_\gamma(q, s) \Gamma_{AAB}^{\gamma\delta}(p, q; -p-q) u_\delta(p, r)|_{p^2=q^2=-m_A^2},$$

$$F_{AA}^{(b1)}(iq_0) \equiv \sum_s \bar{u}_\alpha(p, r) \Gamma_{AAB}^{\alpha\beta}(-p, q; p-q) v_\beta(q, s) G_B(p-q) \\ \times \bar{v}_\gamma(q, s) \Gamma_{AAB}^{\gamma\delta}(p, -q; -p+q) u_\delta(p, r)|_{p^2=q^2=-m_A^2},$$

$$F_{AB}^{(b1-1)}(iq_0) \equiv \bar{u}_\alpha(p, r) \Gamma_{AAB}^{\alpha\beta}(-p, p+q; -q) S_A^{\beta\gamma}(p+q) \\ \times \Gamma_{AAB}^{\gamma\delta}(p, -p-q; q) u_\delta(p, r)|_{p^2=-m_A^2, q^2=-m_B^2},$$

$$F_{AB}^{(b1-2)}(iq_0) \equiv \bar{u}_\alpha(p, r) \Gamma_{AAB}^{\alpha\beta}(-p, p-q; q) S_A^{\beta\gamma}(p-q) \\ \times \Gamma_{AAB}^{\gamma\delta}(p, -p+q; -q) u_\delta(p, r)|_{p^2=-m_A^2, q^2=-m_B^2},$$

$$I_{c1} = -\frac{3}{4\pi L} \int_{-\infty}^{\infty} \frac{dq_0}{2\pi} e^{-L\sqrt{q_0^2+m_A^2}} \{F_{AA}^{(c1)}(iq_0) + F_{AA}^{(c1)}(iq_0)\} + O(e^{-L\bar{m}}), \quad (\text{B.11})$$

$$F_{AA}^{(c1)}(iq_0) \equiv - \sum_s \bar{u}_\alpha(p, r) \Gamma_{AAB}^{\alpha\beta}(-p, p; 0) u_\beta(q, s) \\ \times G_B(0) \bar{u}_\gamma(q, s) \Gamma_{AAB}^{\gamma\delta}(-q, q; 0) u_\delta(p, r)|_{p^2=q^2=-m_A^2},$$

$$F_{AA}^{(c1)}(iq_0) \equiv \bar{u}_\alpha(p, r) \Gamma_{AAB}^{\alpha\beta}(-p, p; 0) v_\beta(q, s) \\ \times G_B(0) \bar{v}_\gamma(q, s) \Gamma_{AAB}^{\gamma\delta}(-q, q; 0) u_\delta(p, r)|_{p^2=q^2=-m_A^2},$$

$$I_{c2} = \frac{3}{4\pi L} \int_{-\infty}^{\infty} \frac{dq_0}{2\pi} e^{-L\sqrt{q_0^2+m_B^2}} F_{AB}^{(c2)}(iq_0) + O(e^{-L\bar{m}}), \quad (\text{B.12})$$

$$F_{AB}^{(c2)}(iq_0) \equiv \bar{u}_\alpha(p, r) \Gamma_{AAB}^{\alpha\beta}(-p, p; 0) u_\beta(p, r) G_B(0) \\ \times \Gamma_{BBB}(0, -q, q)|_{p^2=-m_A^2, q^2=-m_B^2}.$$

The forward scattering amplitudes are defined by



$$F_{AA}(iq_0) = F_{AA}^{(a1)}(iq_0) + F_{AA}^{(b1)}(iq_0) + F_{AA}^{(c1)}(iq_0) , \quad (\text{B.13})$$

$$F_{A\bar{A}}(iq_0) = F_{A\bar{A}}^{(a1)}(iq_0) + F_{A\bar{A}}^{(b1)}(iq_0) + F_{A\bar{A}}^{(c1)}(iq_0) , \quad (\text{B.14})$$

$$F_{AB}(iq_0) = F_{AB}^{(a2)}(iq_0) + F_{AB}^{(b1-1)}(iq_0) + F_{AB}^{(b1-2)}(iq_0) + F_{AB}^{(c2)}(iq_0) . \quad (\text{B.15})$$

## References

- [1] T. Becher and H. Leutwyler, Eur. Phys. J. **C9**, 643 (1999), hep-ph/9901384.
- [2] V. Bernard, T. R. Hemmert, and U.-G. Meissner, Nucl. Phys. **A732**, 149 (2004), hep-ph/0307115.
- [3] M. Procura, T. R. Hemmert, and W. Weise, Phys. Rev. **D69**, 034505 (2004), hep-lat/0309020.
- [4] B. Orth, T. Lippert, and K. Schilling, Nucl. Phys. B (Proc. Suppl.) **129-130**, 173 (2004), hep-ph/0309085.
- [5] G. Colangelo and S. Dürr, Eur. Phys. J. **C33**, 543 (2004), hep-lat/0311023.
- [6] QCDSF-UKQCD Collaboration, A. Ali Khan *et al.*, Nucl. Phys. **B689**, 175 (2004), hep-lat/0312030.
- [7] S. R. Beane, Phys. Rev. **D70**, 034507 (2004), hep-lat/0403015.
- [8] S. R. Beane, Nucl. Phys. **B695**, 192 (2004), hep-lat/0403030.
- [9] M. Lüscher, *On a relation between finite size effects and elastic scattering processes*, Lecture given at Cargese Summer Inst., Cargese, France, Sep 1-15, 1983, DESY 83-116.
- [10] M. Lüscher, Commun. Math. Phys. **104**, 177 (1986).
- [11] P. Hasenfratz and H. Leutwyler, Nucl. Phys. **B343**, 241 (1990).
- [12] G. Höhler, in Landolt-Börnstein, vol. I/9b2, edited by H. Schopper (Springer, Berlin, 1983), p.275, table 2.4.7.1.